JASA ARTICLE

On the tympanic membrane impedance of the katydid *Copiphora gorgonensis* (Insecta: Orthoptera: Tettigoniidae)

Emine Celiker,[1,a)] Thorin Jonsson,[2] and Fernando Montealegre-Z[1,a)]
[1]*School of Life Sciences, University of Lincoln, Joseph Banks Laboratories, Green Lane, Lincoln, LN6 7DL, United Kingdom*
[2]*Institute of Biology, Universitätsplatz 2, Karl-Franzens-University Graz, 8010 Graz, Austria*

ABSTRACT:
Katydids (bush-crickets) are endowed with tympanal ears located in their forelegs' tibiae. The tympana are backed by an air-filled tube, the acoustic trachea, which transfers the sound stimulus from a spiracular opening on the thorax to the internal side of the tympanic membranes (TM). In katydids the sound stimulus reaches both the external and internal side of the membranes, and the tympanal vibrations are then transferred to the hearing organ *crista acustica* (CA) that contains the fluid-immersed mechanoreceptors. Hence the tympana are principally involved in transmitting and converting airborne sound into fluid vibrations that stimulate the auditory sensilla. Consequently, what is the transmission power to the CA? Are the TM tuned to a certain frequency? To investigate this, the surface normal acoustic impedance of the TM is calculated using finite-element analysis in the katydid *Copiphora gorgonensis*. From this, the reflectance and transmittance are obtained at the TM. Based on the impedance results obtained from the pressure recordings at TM and the velocity field calculations in the AT, in the frequency range 5–40 kHz, it is concluded that the tympana have considerably higher transmission around 23 kHz, corresponding to the dominant frequency of the male pure-tone calling song in this species.
https://doi.org/10.1121/10.0002119
(Received 1 June 2020; revised 27 August 2020; accepted 17 September 2020; published online 12 October 2020)
[Editor: Mark A. Bee] Pages: 1952–1960

I. INTRODUCTION

In many species endowed with tympanal ears, the tympanic membrane (TM), also known as the eardrum, is placed at the end of an ear-canal and plays a significant role in transmitting sound waves via tympanal vibrations to the rest of the ear. The intensity of this vibrational transmission to the middle ear depends on the acoustic impedance of the TM. Since any investigation into the middle ear requires information related to the sound vibrations entering this chamber,[1] quantifying the acoustic impedance of the TM becomes important for the characterization of the acoustic qualities of the ear beyond the outer ear.

The transmission power to the middle ear largely depends on the impedance match between the frequency-dependent acoustic impedance of the TM and the frequency-independent characteristic impedance of the ear-canal, which can be calculated if the acoustic impedance of the TM is known. However, there are no commercial systems available that allow for the direct measurement of the TM impedance *in vivo*, leading to the requirement of computational methods for obtaining this important quantity.[2] The aim of this study is to introduce an efficient computational method for obtaining the acoustic impedance of the katydid (bush-cricket) TM, which has been shown to have an analogous hearing system to the mammalian ear.[3]

The acoustic impedance is defined as the measure of the amount of opposition an acoustic pressure system comes across and is calculated through the Fourier transformed signal as the complex ratio between pressure and velocity[4] evaluated at a given point in space and angular frequency. For the normal acoustic impedance of a surface, we would consider the ratio of the average pressure over the surface and the average velocity normal to the surface.

The acoustic impedance of the TM and ear-canal are also instrumental in calculating the reflectance $\mathcal{R}$ and transmittance $\mathcal{T}$, which are the fractions of the incident sound power that are reflected at the TM and transmitted through, respectively,[5] giving quantitative information about the transmission percentage to the middle/inner ear.

The role of the TM in transmitting sound vibrations from the outer ear to the middle ear has been a topic of interest in auditory research for some time for mammalian ears;[1,6–10] however, it has not been investigated in detail for other taxa, especially invertebrates. The acoustically communicating katydids (Orthoptera, Tettigoniidae) also have tympanal ears, located within the proximal part of the tibia in their forelegs [see Figs. 1 and 2(a)]. Each ear is endowed with two TMs, recognised as the anterior tympanic membrane (ATM) and the posterior tympanic membrane (PTM). Unlike most mammalian ears, for katydids the incident pressure waves act on both the external and internal surfaces of the TM,[11,12] so that the TMs function as pressure-difference receivers.[13]

The external input is through the tympanal slits located on the tibiae of the katydid [Figs. 2(c) and 2(d)], and the internal acoustic input is through a tracheal tube (or ear-canal), the acoustic trachea (AT) [Fig. 2(b)], which is

[a)]Electronic mail: eceliker@lincoln.ac.uk and fmontealegrez@lincoln.ac.uk

https://doi.org/10.1121/10.0002119

derived from the respiratory system of the insect.[13–15] The acoustic tracheal system starts at an opening located on the side of the thorax of the insect called the acoustic (auditory) spiracle and runs from the spiracle through the foreleg toward the tibia.[16] In many katydid species, the AT is shaped as an exponential horn: it is comprised of a bulla [see Figs. 2(b) and 2(e)] at the spiracular end that is connected to a narrow tube of almost uniform radius.[14] Adjacent to the terminating end of the tube, located at the proximal part of the fore tibia, lies a collection of mechanoreceptors termed the *crista acustica* (CA),[17] which are connected to the TM at the dorsal wall [see Fig. 2(d)].

It is generally accepted that for katydid species with large auditory spiracles, the main input of sound is the acoustic tracheal system.[18–20] As the sound enters the tracheal tube through the spiracle, it is enhanced as it is transferred to the internal side of the TM.[15,21] This enhancement was first investigated by Michelsen *et al.*,[15] where two species of the genus *Poecilimon* with different sizes of acoustic spiracle and trachea were used to determine the role of these dimensions on pressure gain, finding that in the species with the larger acoustic spiracle the magnitude of the gain was much larger. Further, in the katydid *Copiphora gorgonensis* (Conocephalinae, Copiphorini), for a sound stimulus in the frequency range 23–50 kHz, a pressure gain up to 15 dB has been recorded during internal sound transmission.[22]

There are two main theories related to the acoustical characteristics of the AT, which are both tied to its complex geometry.[11–15,22] The exponential horn theory claims that the AT functions as an exponential horn, which leads to the observed pressure gain of the sound arriving internally. The resonator theory[23] on the other hand, claims that the AT has a resonant frequency that depends on its length. Once the incident wave travels down the AT, however, in both the theories the fraction of the transmitted power to the CA would depend on the TM impedance.

Despite the important function of the TM, there are a limited number of studies on the workings of the TM in katydid ears. Oldfield,[24,25] after conducting experiments by removing the ATM for recording the tuning or the intensity-response characteristics of individual auditory fibres, claimed that the resonant properties of the TM were not responsible for the tuning of the auditory receptors. This claim, however, was contradicted by Kalmring *et al.*[26] and Ross *et al.*[27] Kalmring *et al.*[26] carried out experiments on insects with very thick TM (*Polysarcus denticauda*), and by comparing their recordings to existing data on Tettigoniids with thin TM, they concluded that since the dorsal wall of the AT is directly connected with both TMs, the membranes can be an important link in the transfer of energy to the auditory sensilla of the CA regardless of its thickness. Further, they commented that removing the TM would open the tracheal branches of the receptor organs to the outside air space, which could prevent energy transfer to the receptors.

The workings of the TM were investigated by Nowotny *et al.*[28] for the katydid species *Mecopoda elongata* by analysing the sound-induced vibration pattern of the ATM using a laser Doppler vibrometer (LDV) microscope system. In this study, it was concluded that the higher mode in the vibration pattern may depend on the mechanical impedance of the tympanum plate, which quantifies how much a structure can resist motion if it is subjected to a harmonic force, rather than the acoustic characteristics of the tracheal space below the tympanum.

A numerical investigation of the mechanical processes involved in sound propagation in the AT of the katydid *C. gorgonensis* was also carried out by Celiker *et al.* (2020).[29] After conducting a model sensitivity analysis that took into account the acoustic impedance of the TM, it was concluded that even though the AT geometry was the major factor in the observed pressure gain, the TM acoustic impedance also played a role in this.

In this study, we further numerically investigate the surface normal acoustic impedance of the TM of *C. gorgonensis* using the precise 3D geometry of the AT that is obtained from micro-computed tomography (μ-CT) and 3D reconstruction [see Fig. 2(e)]. For the remainder of the paper, we refer to the acoustic impedance when impedance is mentioned. With the use of the obtained TM impedance results, we also calculate the values of $\mathcal{R}$ and $\mathcal{T}$. These values have so far not been determined but will provide an important basis for further studies on the mechano-acoustic system of katydids, since they provide information about the power intensity entering the CA. Due to the analogy between katydid and mammalian ears,[3] this in turn can also serve to further understand and model the mammalian hearing system. The impedance results also have an important application in obtaining realistic models with accurate mechanical parameters for simulating sound propagation in the AT.

Based on our numerical results for the surface normal impedance, $\mathcal{R}$ and $\mathcal{T}$, we test our hypothesis that the transmission power from the TM is optimal at the *C. gorgonensis* calling song frequency, which is 23 kHz, and we discuss the general frequency-dependent transmission power to the CA through the TM.

II. MATERIALS AND METHODS

A. Experimental animals

For the conducted experiments and numerical simulations, three specimens (one male, two females) of the katydid species *C. gorgonensis* were used, which are endemic to the island of Gorgona, Colombia. Collected as nymphs, the specimens were kept in cages at 25 °C, a light/dark cycle of 11/13 h, and 70% relative humidity. Their diet during this captivity consisted of a mix of pollen, dry cat food, and water.

Once the specimens reached adulthood, they were used for various LDV experiments, for instance in the experiment described in Sec. II B and in Jonsson *et al.* (2016),[22] and generally survived these experiments. Upon their natural death, the specimens' bodies were preserved by injecting

2 ml of Bouin's solution. The same number of specimens were used for 3D μ−CT scanning as described in Sec. II C.

B. Experimental setup

a. Apparatus and calibration. The preparation was positioned on a Melles Griot Optical Table Breadboard, Pneumatic Vibration Isolation (1 × 1 m area) (Melles Griot; Rochester, NY), along with the LDV (Polytec PSV-500-F; Waldbronn, Germany). A loudspeaker (Ultrasonic Dynamic Speaker Vifa; Avisoft Bioacoustics) with a custom-designed plastic probe adapter was positioned at 2 mm away from the spiracle ipsilateral to the ear examined (see Fig. 1). This procedure has been described in detail in Jonsson *et al.* (2016)[22] and Montealegre-Z *et al.* (2012).[22] The probe speaker made it difficult to flatten the spectrum, therefore sound was delivered without amplitude correction for each frequency, and pressure was measured using a 1/8 inch precision pressure microphone (Brüel & Kjær, 4138; Nærum, Denmark) and a preamplifier (Brüel & Kjær, 2633), placed at 2 mm away from the probe tip. The microphone's sensitivity was calibrated using a sound level calibrator (Brüel & Kjær, 4231).

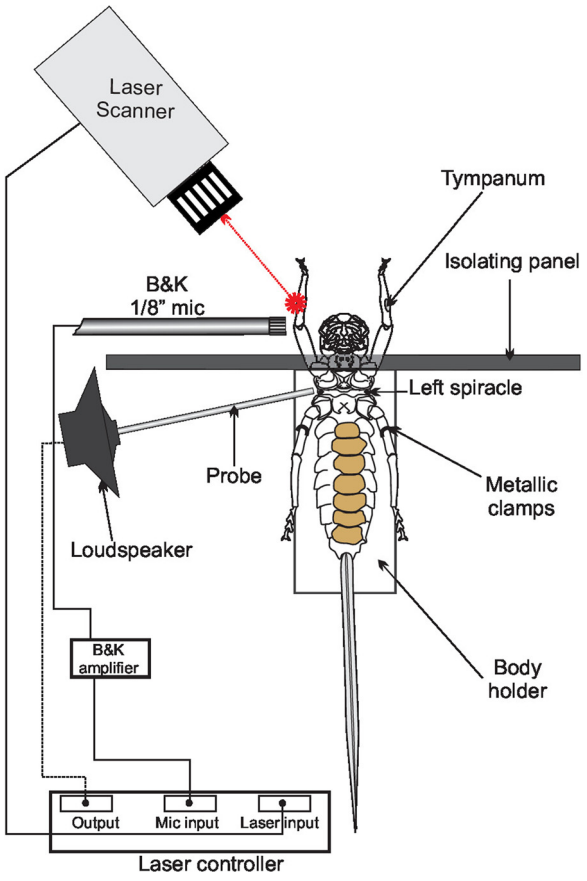

FIG. 1. (Color online) The experimental procedure for obtaining the pressure recording on the tympanic membrane. An isolating panel is used to ensure the sound stimulus reaches the tympanic membrane only from the acoustic trachea.

b. Acoustic stimulation and vibration recordings. The TM was acoustically stimulated via the AT only, using a probe loudspeaker and a platform that allows the isolation and control of external and internal ear inputs.[3,22] In this case sound was delivered to the acoustic spiracle only using the probe speaker, preventing any external sound pressure from reaching the TM or the leg cuticle (see Fig. 1).

The stimulus consisted of periodic chirps with a changing frequency covering the interval 5–50 kHz, and the overall duration of a full chirp was 32 milliseconds, with a resolution of 1.95 μs (at a sampling rate of 512 kHz). A ramp was not used for the periodic chirps. The stimulus chirps were generated from the Polytec software (PSV 9.2), passed to an amplifier (A-400, Pioneer, Kawasaki, Japan), and sent to the loudspeaker. The vibration velocity of the TM was measured using the LDV with a PSV-A-410 close-up unit. The mechanical responses were analysed by simultaneously recording the vibration velocity of the TM, and the sound stimulus measured at the auditory spiracle. The tympanal slits of the specimens were left intact, leaving only a narrow slit to focus the laser beam on the tympanal surface. Therefore, the entire TM could not be scanned, instead the laser scanner LDV was operated to record vibrations using single-shot mode. The data thus collected enabled us to calculate magnitude/frequency transfer functions of the tympanal response when the ear was stimulated only through the AT path.

Transfer functions were computed directly in the Polytec software, which employs the formula

$$H(f) = \frac{Y(f)}{X(f)},$$

where $H(f)$ = transfer function, $Y(f)$ = output of the system in the frequency domain, and $X(f)$ = input of the system in the frequency domain. Since the probe speaker was put 2 mm away from the spiracle, this gave us some space to place the 1/8 inch microphone beside the tip of the probe, while leaving enough space for sound to enter the spiracle. We also recorded the stimulus separately (as time signal) by putting the microphone 2 mm away from the probe speaker tip. We did not find any difference in the magnitude and phase using either the Polytec automatic method, or MATLAB manual calculations.

C. μ-CT description and segmentation

X-ray μ-CT and 3D reconstruction were used to obtain the precise AT geometry. This was achieved with the use of standard biomedical imaging software, with the same procedure as outlined in Jonsson *et al.* (2016).[22] The animals were euthanised using ethyl ethanoate and immediately scanned without any further fixation of tissues. μ-CT images were obtained with a Bruker Skyscan 1272 (Bruker microCT; Kontich, Belgium) at 100 kV, 36 μA with a 0.5 mm thick aluminium filter and between 0.2° and 0.4° rotation steps between images, resulting in a pixel resolution of $\approx$ 11 μm. Scan times varied among specimens (due to

https://doi.org/10.1121/10.0002119

positioning of the animals and the region to be scanned in order to capture the entirety of the legs, head, and thorax) between 25 and 45 min. The 3D reconstruction of the AT was carried out with AMIRA (v. 6.7.0, Thermo Fisher Scientific) and exported as STL files, which were further processed after being imported into Comsol Multiphysics (v 5.5, Comsol, Inc.; Burlington, MA, USA).

D. Impedance calculation

For calculating the surface normal impedance, we applied the formula[30]

$$\langle Z_n \rangle_{TM} = \frac{\langle p \rangle_{TM}}{\langle u_n \rangle_{TM}}, \tag{1}$$

where $\langle \cdot \rangle_{TM}$ denotes the ensemble average on TM, $p = p(\mathbf{x}; \omega)$ is the harmonic pressure at the point $\mathbf{x} = \{x_1, x_2, x_3\}$ and the angular frequency ω, and $u_n(\mathbf{x}; \omega) = \mathbf{u}(\mathbf{x}; \omega) \cdot \mathbf{n}$ is the dot product of the velocity $\mathbf{u}$ with the normal vector $\mathbf{n}$ to the surface.

The impedance $\langle Z_n \rangle_{TM}$ is a complex quantity which can be defined as

$$\langle Z_n \rangle_{TM} = Z_1 + jZ_2, \tag{2}$$

where Z_1 and Z_2 are the resistance and reactance, respectively, and $j = \sqrt{-1}$. Traditionally, *resistance* is defined as the property of the material that opposes the applied pressure, whereas *reactance* is the opposition encountered by the pressure field that is also dependent on the frequency of the sound wave.[5]

Since the median diameter of the AT is approximately 300 μm,[22] it is small enough to consider only uniform plane waves in the tube. On the basis of this assumption, we obtained the average pressure by using experimental pressure data on the TM. The average normal velocity has been calculated numerically by simulating the propagation of sound in the 3D geometry of the AT, as it is not possible to obtain this experimentally. Once the average pressure and normal velocity are known, from continuity it follows that the surface normal impedance can be obtained by Eq. (1).

The 3D geometry of the AT used for the simulations is demonstrated in Fig. 2(e). Due to computational difficulties, the narrowing end of the tube is cut off right at the start of the TM and an artificial TM is placed at the end of the AT.

The mathematical model used for the simulation takes into account the thermal and viscous losses encountered in narrow tubes, which lead to the attenuation of the sound waves. For the fluid domain (i.e., inside of the gas-filled AT), the governing equations are the fully linearized Navier-Stokes equation, the continuity equation, and the energy conservation equation, which are solved in the frequency domain. The properties of the gas inside the tube are not precisely known; however, it is believed to be mostly air. Hence we have assumed that the gas inside the tube is air for the simulations.

Further, the tracheal wall is known to be made of sclerotised chitin. As reported by Vincent and Wegst,[31] such a

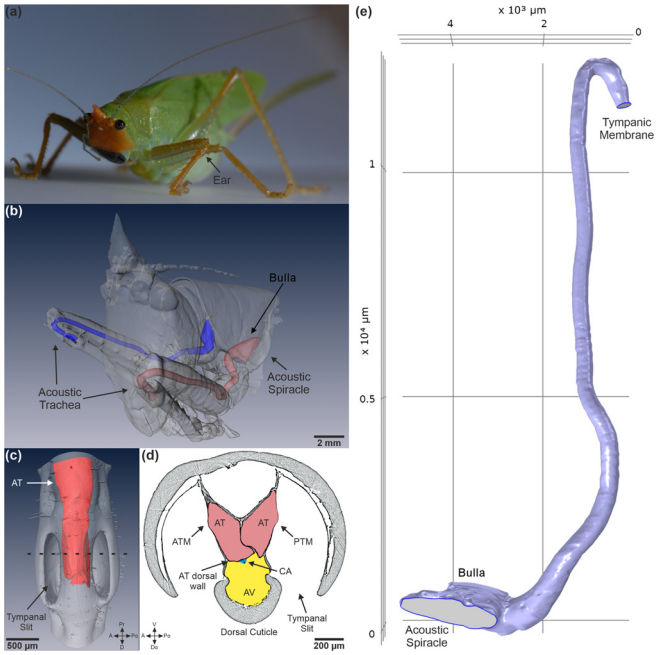

FIG. 2. (Color online) The ear morphology of the katydid *Copiphora gorgonensis*. (a) A female *C. gorgonensis*. (b) Semi-transparent model on the basis of μ-CT data from (a) showing the acoustic tracheae in red (left AT) and blue (right AT). (c) The magnified left ear from (b) showing the AT and the tympanal slits. (d) A cross-section of the left ear along the dashed line in (c). (e) FEM model of a right AT as used in the simulations. A = anterior, AT = acoustic trachea, ATM = anterior tympanic membrane, AV = acoustic vesicle, CA = crista acustica, D = distal, Do = dorsal, Po = posterior, Pr = proximal, PTM = posterior tympanic membrane, V = ventral.

structure has Young's modulus in the range 1–20 GPa and density between 1000 and 1300 kg/m^3. With this information, the interaction between the fluid and the AT wall can also be accounted for in the model. This is achieved by coupling the equations in the fluid domain with the elastic Helmholtz equation, whose solution represents the displacements in the wall. The exact values for the material properties of the AT wall are not known, however, it has been demonstrated that changes in the Young's modulus and density in the above ranges have no significant effect on the observed pressure gain at the TM.[29] We therefore have chosen the same values as used in Celiker *et al.*, 2020[29] (see Table I for the parameter values used in the mathematical model). As a simplifying assumption, we have assumed that the AT wall is built of an isotropic, incompressible, and homogeneous material. The mean AT wall thickness, which

TABLE I. Parameter values used in the mathematical model simulating sound propagation in the AT.

Parameter	Value
AT Wall - Young's Modulus	1.7 GPa
AT Wall - Poisson's Ratio	0.3
AT Wall - Density	1300 kg/m^3
Mean AT Wall Thickness	13 μm
Equilibrium Temperature	293.15 K
Equilibrium Pressure	1 atm

has been obtained through μ-CT measurements to be 13 μm (data not shown), is also incorporated into the model. Finally, we assume that adiabatic thermal processes are taking place in the system. The described system of equations is outlined in the Appendix.

For the simulation, a harmonic incident wave is modelled, entering the tube through the spiracle. This wave has the magnitude of the sound stimulus used during the experiments outlined in Sec. II B. The frequency of the incident wave is taken to be in the interval 5–40 kHz with a resolution of 62.5 Hz. At the TM, for the boundary condition we construct a linear interpolation function for the frequency dependent pressure magnitude, which contains the experimental data obtained on the TM.

For the finite-element solution of the obtained system of equations, the mesh is constructed as in Celiker *et al.* (2020).[29] The maximum element size has been chosen such that there are at least 10 finite elements per wavelength. Furthermore, boundary layer elements are employed in the vicinity of the AT wall to resolve the thermal and viscous boundary layers formed in the solution near the wall, which lead to thermal and viscous losses. These were connected with the AT wall elements of the mixed interpolation of tensorial components type,[32] which are used for modelling different behaviors of thin structures with various stress conditions.

We request a third-order accurate finite element solution (in the L_2-norm) by basing the solution on quadratic Lagrange elements.[33] The system of finite element equations was solved by the thermoviscous acoustics-shell interaction module of the commercial software Comsol Multiphysics v.5.5.[34]

The calculation of the normal impedance from Eq. (1) was also carried out in Comsol Multiphysics, after computing the velocity vector on the TM. The ensemble average, $\langle\cdot\rangle_{TM}$, was obtained by a fourth-order integration approximation over the artificial TM, using the in-built integration operator. Hence for calculating the numerator of Eq. (1), experimentally obtained pressure recordings on the TM were averaged using this operator. Likewise for the denominator of Eq. (1), the integration operator was applied after taking the dot product of the calculated velocity vector on the TM with the normal vector to the TM, where the normal vector was obtained precisely using Comsol Multiphysics.

To compute the reflection coefficient R we use the formula[4,5]

$$R = \frac{\langle Z_n\rangle_{TM}/Z_0 - 1}{\langle Z_n\rangle_{TM}/Z_0 + 1}, \tag{3}$$

where $Z_0 = \rho c$ is the average characteristic impedance of a cross-sectional area of the tube, ρ and c are air density and speed of sound in air, respectively. Hence for the characteristic impedance we make the simplifying assumption that there are no losses in the tube.

From formula (3), the power reflectance is calculated as[5]

$$\mathcal{R} = |R|^2, \tag{4}$$

from which the percentage of the power magnitude that's reflected at the TM ($100 \times \mathcal{R}\%$) can be calculated.

Using Eq. (4), we also calculate the power transmittance $\mathcal{T}$ through the TM by using the relation[5]

$$1 = \mathcal{R} + \mathcal{T}. \tag{5}$$

III. RESULTS

The surface normal impedance $\langle Z_n\rangle_{TM}$, for the TM of one male and two female *C. gorgonensis* has been calculated as described in Sec. II D.

The results obtained for the mean and standard deviation (SD) of the resistance and reactance of the TM impedance for three *C. gorgonensis* specimens (one male, two females), in the frequency range 5–40 kHz are presented in Fig. 3. From Fig. 3, it can be observed that both the resistance and reactance have the highest magnitude at 5 kHz. Using the notation from Eq. (2), mean $Z_1 = 1130.3$ ($\pm$ 833 SD) Pa · s/m in the left trachea, and $Z_1 = 1399.2$ ($\pm$ 451 SD) Pa · s/m in the right trachea. These values also peak around 20 kHz, where mean $Z_1 = 849.7$ ($\pm$660.42 SD) Pa · s/m at 20.625 kHz in the left trachea, and mean $Z_1 = 1153.67$ ($\pm$923.68) Pa · s/m at 19.938 kHz in the right trachea.

The experimental data for the TM acoustic impedance of *C. gorgonensis* (or other katydid species) is not available in the literature. Hence, we have used the response of the TM obtained with the laser as displacement per unit pressure, described in Sec. II B, to verify our results by simulating the propagation of sound in the AT with the calculated impedance values. The obtained numerical sound pressure

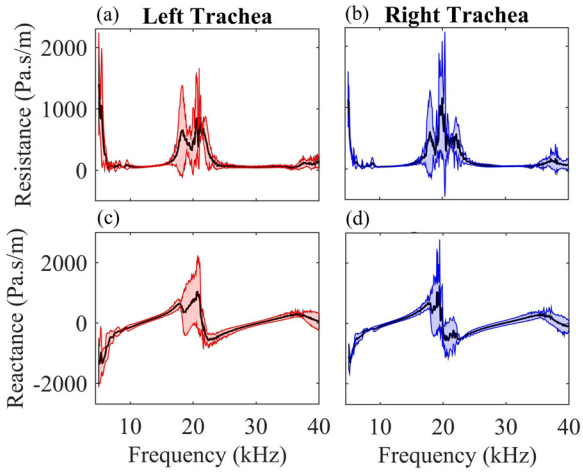

FIG. 3. (Color online) The resistance and reactance. The resistance (real part) of the calculated surface normal impedance for the tympanic membrane in the (a) left trachea and the (b) right trachea. The reactance (imaginary part) in the (c) left trachea and the (d) right trachea of the calculated surface normal impedance. The black curves represent the mean obtained from one male and two female specimens, and the shaded areas refer to the standard deviation.

https://doi.org/10.1121/10.0002119

level (SPL) results on the TM are then compared to the experimental data. The mean and SD of the absolute error between the experimental and numerical results are presented in Fig. 4. The mean maximum differences between the experimental and numerical results are 7.7147 dB and 6.858 dB on the TM of the left and right AT, respectively, which demonstrate the high accuracy of the results.

With the use of the calculated impedance values, the magnitudes of the power reflectance $\mathcal{R}$ and the power transmittance $\mathcal{T}$ have also been calculated by Eqs. (4) and (5), respectively, for each specimen, and converted to percentages (see Figs. 5 and 6). From the obtained results, at the lower frequencies of 5–10 kHz, there is no specific correlation between frequency and reflectance/transmittance. The largest transmission appears to be around the resonant frequency of 23 kHz, with a mean transmission of 40%–90% for 19.8–23.19 kHz in the left AT and 47%–78% for 18.5–24.625 kHz in the right AT. An increase in the mean transmission was also observed in the interval 37–40 kHz, where the maximum mean transmission in this interval was 56.7% at 39.7 kHz in the left AT and 54.2% at 37 kHz in the right AT. For the remainder of the frequency interval, there is a uniform rate of mean reflection and transmission of approximately 70% to 30%, respectively. Our results support our hypothesis that for the katydid species *C. gorgonensis*, optimal transmittance is obtained at the calling frequency.

IV. DISCUSSION

In this study, we set out to calculate the impedance of the TM for the katydid *C. gorgonensis* on the basis of real-life experiments coupled with finite-element simulations of sound propagation in the AT. Using the sound pressure measurements obtained experimentally on the TM, a coupled system of equations is solved in the constructed 3D AT geometry accounting for the thermal and viscous losses in the tube, as well as the interaction of the gas inside the tube with the elastic wall of the AT.

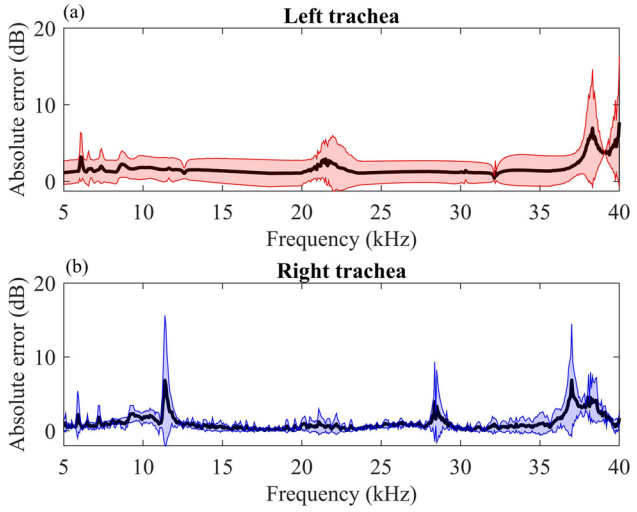

FIG. 4. (Color online) The absolute error. The absolute error between the experimental and numerical results from (a) the left trachea and (b) the right trachea. The black curves represent the mean obtained from one male and two female specimens, and the shaded areas refer to the standard deviation.

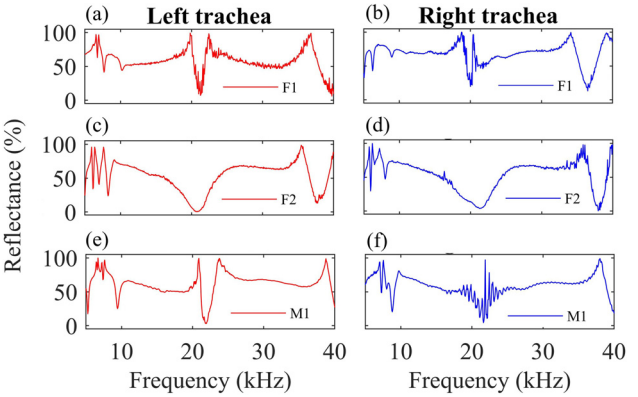

FIG. 5. (Color online) Power reflectance percentage from the tympanic membrane. The percentage of power reflectance $\mathcal{R}$ from the left trachea [panels (a), (c), and (e)] and the right trachea [panels (b), (d), and (f)], for two female (F1 and F2) and one male (M1) specimens.

The results we present are based on the mean and SD of three specimens (one male, two females), and hence three left AT and three right AT. For the frequency range 5–40 kHz, our results show that the real and imaginary parts of the TM normal impedance have the largest magnitudes around 5 kHz (see Fig. 3). For 7–40 kHz, the mean magnitude is about 50–250 Pa · s/m for both the resistance and reactance, with the exception of around 20 kHz where they show a secondary peak (Fig. 3).

For mammals and some non-mammalian tetrapods alike, for the largest transmission of the sound wave from the ear-canal, there should be an impedance match between the TM impedance (terminating impedance of the tube) and the frequency-independent characteristic impedance of the ear-canal. By definition, the power reflectance demonstrated in Fig. 5 shows the percentage of the impedance mismatch between the TM surface normal impedance $\langle Z_n \rangle_{TM}$ and the AT characteristic impedance Z_0 for *C. gorgonensis*, from which it can be inferred that the

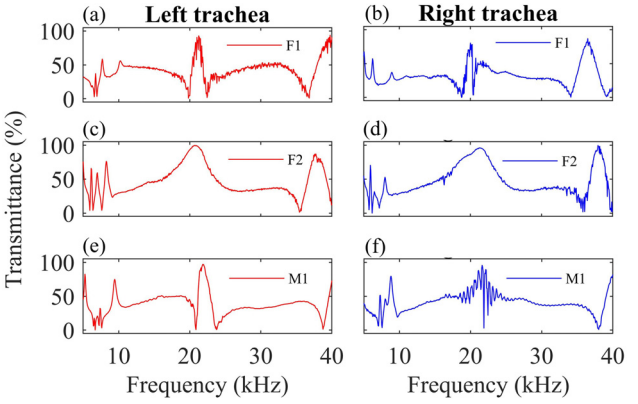

FIG. 6. (Color online) Power transmittance percentage from the tympanic membrane. The percentage of power transmittance $\mathcal{T}$ from the left trachea [panels (a), (c), and (e)] and the right trachea [panels (b), (d), and (f)], for two female (F1 and F2) and one male (M1) specimens.

smallest rate of power reflection is around 23 kHz. By Eq. (5), this means that the largest power transmission is around this frequency (see Fig. 6).

The frequency 23 kHz is significant for *C. gorgonensis* since it is the intra-specific frequency for the species' social communication and mating calls.[22] From $\mathcal{R}$ and $\mathcal{T}$ it can be easily calculated that around 23 kHz the reflected wave magnitude is very small (a mean value of 17% at 21.8 kHz in the left AT and 20% at 21.6 kHz in the right AT), and thus the transmission magnitude of the wave to the CA is around 80%, compared to the approximately 30% transmission of the sound waves in the remainder of the range 7–37 kHz. The transmission also peaks in the interval 37–40 kHz, however the mean transmission in this interval remains less than 60% for both the left and right AT, suggesting that *C. gorgonensis* is more sensitive to sound at 23 kHz. Hence, the obtained results indicate that our hypothesis, which states that for *C. gorgonensis* there is a higher transmission from the TM at their calling frequency of 23 kHz, holds true. To test if this conclusion also holds for different katydid species, we will conduct a species comparison study to investigate whether the power transmittance of signals from the AT are likewise optimal at frequencies that are important for the survival of the species in question.

From Figs. 5 and 6, it can also be observed that even though there is consistently optimal transmission at the *C. gorgonensis* calling frequency, in the neighbouring frequency band (15–25 kHz) the reflectance and transmission is varying independently of frequency. Since there might be no requirement for this species to exhibit high accuracy or mechanical acuity in the periphery of 23 kHz for their survival, the variability of the data could be attributed to the hearing system being less developed for frequency determination or discrimination at frequencies outside of their calling song range (at least in the frequency range examined here). Another factor leading to the difference in transmittance can also be attributed to the inherent variability of biological systems due to developmental factors such as size, age, and sex, which would require a larger sample size for further investigation.

However, we approach the physical interpretations of the results very cautiously since the calculations are based on the tracheal input (the main sound input for this species), and the model does not account for the external sound input, and hence for the mechanical properties of the tympanal flaps (or pinnae) located adjacent to the TM. Nevertheless, as demonstrated in Fig. 4, the numerical results for impedance give a good approximation for the sound pressure magnitude on the TM and are effective for simulating the propagation of sound in the AT. In addition, knowledge about the TM acoustic impedance enables researchers to model the sound behaviour in the CA more accurately and separately from the remainder of the ear, as the power intensity of the vibrational stimulus entering this chamber can be obtained from the transmittance.

The acoustic impedance of the TM and ear-canal has also been a topic of interest for the mammalian ear,[16–20] since it provides significant information about the power transmission into the middle ear. However, as there is no technique for measuring the average velocity directly on the TM,[6] in many studies, especially those investigating mammalian hearing, indirect methods have been used for calculating the acoustic impedance. Some of these indirect methods include using sound wave reflection measurements to obtain the impedance by taking recordings of the pressure reflectance magnitude at a certain distance from the TM,[7] or applying numerical methods that would only require the pressure magnitude obtained at different locations along the ear-canal.[6] However, as stated by Voss and Allen,[7] many of these studies faced the following problems:

(1) Unknown canal length from the measurement point to the TM.
(2) Cross-sectional area changes in the canal as a function of distance.
(3) Complicated geometry of the TM.

Another challenge to the numerical methods for calculating the TM impedance was taking into account the thermal and viscous losses in the system.[6,8] As our solutions use the 3D geometry of the AT obtained through μ-CT, we largely overcome the issues related to the complex geometry of the AT. Using the sound pressure measurements obtained experimentally on the TM has also enabled us to avoid the issue of the unknown measurement point from the TM in the ear-canal. Moreover, our mathematical model takes into account the thermal and viscous losses in the AT.

However, some simplifications had to be made to the TM geometry due to computational requirements. Constructing a stable finite-element mesh at the distal and narrowing end of the AT was problematic, and hence to overcome this, we cut off the part of the AT right at the start of the TM and constructed an artificial TM at the end of the tube. Since the AT median radius is 150 μm,[22] the tube is narrow enough to consider only uniform plane waves. The sound field in the AT was also numerically demonstrated to be longitudinal standing waves by Celiker *et al.*[29] Hence, by the continuity of the system and on the assumption that the sound wave inside the AT is a longitudinal wave, the use of an artificial TM placed exactly at the first point of contact of the incident wave with the actual TM will not lead to significant discrepancies in the results.

On the assumption that the ear-canal geometry is known, for instance through a medical CT of the head, the coupled system of equations used in this paper can also be applied for the numerical calculation of the mammalian TM impedance, which will reduce the problems related to the losses in the tube, as well as having to take sound pressure recordings at potentially hard to locate positions along the ear-canal.

ACKNOWLEDGMENTS

E.C. and F.M.Z. are funded by the European Research Council, Grant No. ERCCoG-2017-773067, awarded to

https://doi.org/10.1121/10.0002119

F.M.Z. for the project "The Insect Cochlea." T.J. is supported through the European Commission via a Horizon 2020 Marie Skłodowska-Curie fellowship (No. 829208, InWingSpeak). Specimens were collected under the research permit No. DIG 009-14 and were brought to the UK with the export permit No. COR 5494-14, issued by the Administrative Unit of National Natural Parks of Colombia. The experimental procedure followed in this study has been approved by the ethics regulations of the University of Lincoln, under the project "The Insect Cochlea" (Ethics Reference No. 2019-May-0160).

APPENDIX: THE MATHEMATICAL MODEL

Let Ω denote the AT of *C. gorgonensis*, such that Ω_f is the inside of the AT (the fluid domain), Ω_s is the wall of the AT (the solid domain), and $\gamma = \Omega_s \cap \Omega_f$. Further, γ_1 denotes the acoustic spiracle, γ_2 is the artificial tympanic membrane, and γ_3 is the outer boundary of Ω_s so that $\Omega = \Omega_f \cup \Omega_s \cup (\cup_{i=1}^{3}\gamma_i)$.

The following system of equations is considered on Ω:

$$0 = i\omega\rho + \nabla\cdot(\rho_0\mathbf{u}_f) \text{ on } \Omega_f, \tag{A1}$$

$$i\omega\rho\mathbf{u}_f = \nabla\cdot\left[-pI + \mu(\nabla\mathbf{u}_f + (\nabla\mathbf{u}_f)^T) - \left(\frac{2\mu}{3} - \mu_B\right)(\nabla\mathbf{u}_f)I\right] \text{ on } \Omega_f, \tag{A2}$$

$$T = \frac{\alpha_0 T_0}{\rho_0 C_p} p \text{ on } \Omega_f, \tag{A3}$$

$$\rho = \rho_0(\beta_T p - \alpha_0 T) \text{ on } \Omega_f, \tag{A4}$$

$$p = p_0 \text{ on } \gamma_1, \tag{A5}$$

$$-p_0\mathbf{n} = \left[-pI + \mu(\nabla\mathbf{u}_f + (\nabla\mathbf{u}_f)^T) - \left(\frac{2\mu}{3} - \mu_B\right)(\nabla\mathbf{u}_f)I\right]\mathbf{n} \text{ on } \gamma_1, \tag{A6}$$

$$p = \mathcal{L}(\omega/2\pi) \text{ on } \gamma_2, \tag{A7}$$

$$-\mathcal{L}(\omega/2\pi)\mathbf{n} = \left[-pI + \mu(\nabla\mathbf{u}_f + (\nabla\mathbf{u}_f)^T) - \left(\frac{2\mu}{3} - \mu_B\right)(\nabla\mathbf{u}_f)I\right]\mathbf{n} \text{ on } \gamma_2, \tag{A8}$$

$$\mathbf{0} = -\rho_s\omega^2\mathbf{U}_s - \nabla\cdot\sigma(\mathbf{U}_s) \text{ on } \Omega_s, \tag{A9}$$

$$0 = \sigma_{ij}\cdot n_j,\ i,j = 1,2,3 \text{ on } \gamma_3, \tag{A10}$$

$$\mathbf{u}_f = i\omega\mathbf{U}_s \text{ on } \gamma, \tag{A11}$$

$$0 = -\mathbf{n}\cdot(-k\nabla T) \text{ on } \gamma. \tag{A12}$$

On Ω_f, Eqs. (A1)–(A4) are the continuity equation, the linearized Navier-Stokes equations, the energy equation, and the linearized equation of state, respectively; $\omega =$ angular frequency; $\rho =$ density; $\rho_0(p_0, T_0) =$ equilibrium density; $\mu =$ dynamic viscosity; $\mu_B =$ bulk viscosity; $C_p =$ heat capacity at constant pressure; $T_0 =$ equilibrium temperature; $p_0 =$ equilibrium pressure; $I =$ identity matrix; $\alpha_0 =$ coefficient of thermal expansion; and $\beta_T =$ the isothermal compressibility obtained from the speed of sound in the considered fluid. The dependent variables are $p =$ pressure, $\mathbf{u}_f =$ velocity, and $T =$ temperature. The values of $\rho_0, \mu, \mu_b, C_p, \alpha_0$, and β_T are taken as properties of air at 20 °C.

For the boundary conditions in Eqs. (A5)–(A8), p_0 is the amplitude of the sound wave entering the AT from γ_1, and on γ_2 we apply $\mathcal{L}(\omega/2\pi)$, which is a linear interpolation function giving the pressure magnitude recorded on the TM experimentally at the input frequency.

The elastic Helmholtz Eq. (A9) is applied on Ω_s, where $\rho_s =$ wall density, $\sigma_{ij} = E/1+\nu\epsilon_{ij} + E\nu/(1+\nu)(1-2\nu)\epsilon_{kk}\delta_{ij},\ i,j = 1,2,3, E =$ Young's modulus; $\nu =$ Poisson's ratio, $0 < \nu < 1/2; \epsilon_{ij} = \frac{1}{2}(\partial\mathbf{U}_{si}/\partial x_j + \partial\mathbf{U}_{sj}/\partial x_i)$ the strain tensor and $\delta_{ij} =$ the Kronecker-delta function. The dependent variable $\mathbf{U}_s$ represents the displacement vector of the wall. By the boundary condition in Eq. (A10), no external stress is applied on γ_3.

Finally the fluid and solid systems are coupled on γ by Eqs. (A11) and (A12), where $k =$ thermal conductivity and the complex number $i = \sqrt{-1}$.

[1]H. Hudde, A. Engel, and A. Lodwig, "Methods for estimating the sound pressure at the eardrum," J. Acoust. Soc. Am. **106**(4), 1977–1992 (1999).
[2]J. B. Allen, "Measurement of eardrum acoustic impedance," in *Peripheral Auditory Mechanisms* (Springer, Berlin, Heidelberg, 1986), pp. 44–51.
[3]F. Montealegre-Z, T. Jonsson, K. A. Robson-Brown, M. Postles, and D. Robert, "Convergent evolution between insect and mammalian audition," Science **338**(6109), 968–971 (2012).
[4]S. W. Rienstra and A. Hirschberg, *An Introduction to Acoustics*. (Eindhoven, University of Technology, 2004), **18**, 19.
[5]L. E. Kinsler, A. R. Frey, A. B. Coppens, and J. V. Sanders, *Fundamentals of Acoustics*, 4th ed. (Wiley-VCH, Weinheim, Germany, 1999).
[6]H. Hudde, "Measurement of the eardrum impedance of human ears," J. Acoust. Soc. Am. **73**(1), 242–247 (1983).
[7]S. E. Voss and J. B. Allen, "Measurement of acoustic impedance and reflectance in the human ear canal," J. Acoust. Soc. Am. **95**(1), 372–384 (1994).
[8]H. Hudde, "Estimation of the area function of human ear canals by sound pressure measurements," J. Acoust. Soc. Am. **73**(1), 24–31 (1983).
[9]A. S. Feldman, "Impedance measurements at the eardrum as an aid to diagnosis," J. Speech Hear. Res. **6**(4), 315–327 (1963).
[10]M. E. Ravicz, E. S. Olson, and J. J. Rosowski, "Sound pressure distribution and power flow within the gerbil ear canal from 100 Hz to 80 kHz," J. Acoust. Soc. Am. **122**(4), 2154–2173 (2007).
[11]R. Heinrich, M. Jatho, and K. Kalmring, "Acoustic transmission characteristics of the tympanal tracheae of bushcrickets (Tettigoniidae). II: Comparative studies of the tracheae of seven species," J. Acoust. Soc. Am. **93**(6), 3481–3489 (1993).
[12]J. X. Shen, "A peripheral mechanism for auditory directionality in the bushcricket *Gampsocleis gratiosa*: Acoustic tracheal system," J. Acoust. Soc. Am. **94**(3), 1211–1217 (1993).
[13]O. N. Larsen, "Mechanical time resolution in some insect ears," J. Compar. Physiol. **143**(3), 297–304 (1981).
[14]E. Hoffmann and M. Jatho, "The acoustic trachea of tettigoniids as an exponential horn: Theoretical calculations and bioacoustical measurements," J. Acoust. Soc. Am. **98**(4), 1845–1851 (1995).

[15]A. Michelsen, K. Rohrseitz, K. G Heller, and A. Stumpner, "A new biophysical method to determine the gain of the acoustic trachea in bushcrickets," J. Compar. Physiol. A **175**(2), 145–151 (1994).
[16]W. J. Bailey, *Acoustic Behaviour of Insects: An Evolutionary Perspective*. (Chapman and Hall Ltd., London, 1991).
[17]W. Rössler, M. Jatho, and K. Kalmring, "The auditory–vibratory sensory system in bushcrickets," in *Insect Sounds and Communication* (CRC Press, Boca Raton, FL, 2005), pp. 45–79.
[18]D. B. Lewis, "The physiology of the Tettigoniid ear: I. The implications of the anatomy of the ear to its function in sound reception," J. Exper. Biol. **60**(3), 821–837 (1974).
[19]K. G. Hill and B. P. Oldfield, "Auditory function in Tettigoniidae (Orthoptera: Ensifera)," J. Compar. Physiol. **142**(2), 169–180 (1981).
[20]K. Kalmring, W. Rössler, and C. Unrast, "Complex tibial organs in the forelegs, midlegs, and hindlegs of the bushcricket *Gampsocleis gratiosa* (Tettigoniidae): Comparison of the physiology of the organs," J. Exper. Zool. **270**(2), 155–161 (1994).
[21]A. Stumpner and K. G. Heller, "Morphological and physiological differences of the auditory system in three related bushcrickets (Orthoptera: Phaneropteridae, *Poecilimon*)," Physiol. Entomol. **17**(1), 73–80 (1992).
[22]T. Jonsson, F. Montealegre-Z, C. D. Soulsbury, K. A. Robson Brown, and D. Robert, "Auditory mechanics in a bush-cricket: Direct evidence of dual sound inputs in the pressure difference receiver," J. R. Soc. Interface **13**(122), 20160560 (2016).
[23]H. Nocke, "Physical and physiological properties of the Tettigoniid ("grasshopper") ear," J. Compar. Physiol. **100**(1), 25–57 (1975).
[24]B. P. Oldfield, "Short communication: The role of the tympanal membranes in the tuning of auditory receptors in Tettigoniidae (Orthoptera: Ensifera)," J. Exper. Biol. **116**(1), 493–497 (1985).
[25]B. P. Oldfield, "Tonotopic organisation of auditory receptors in Tettigoniidae (Orthoptera: Ensifera)," J. Compar. Physiol. **147**(4), 461–469 (1982).
[26]K. Kalmring, E. Hoffmann, M. Jatho, T. Sickmann, and M. Grossbach, "The auditory–vibratory sensory system of the bushcricket *Polysarcus denticauda* (Phaneropterinae, Tettigoniidae) II. Physiology of receptor cells," J. Exper. Zool. **276**(5), 315–329 (1996).
[27]W. Rössler, A. Hübschen, J. Schul, and K. Kalmring, "Functional morphology of bushcricket ears: Comparison between two species belonging to the Phaneropterinae and Decticinae (Insecta, Ensifera)," Zoomorph. **114**(1), 39–46 (1994).
[28]M. Nowotny, J. Hummel, M. Weber, D. Möckel, and M. Kössl, "Acoustic-induced motion of the bushcricket (*Mecopoda elongata*, Tettigoniidae) tympanum," J. Compar. Physiol. A **196**(12), 939–945 (2010).
[29]E. Celiker, T. Jonsson, and F. Montealegre-Z, "The auditory mechanics of the outer ear of the bush cricket: A numerical approach," Biophys. J. **118**(2), 464–475 (2020).
[30]T. Otsuru, R. Tomiku, N. B. C. Din, N. Okamoto, and M. Murakami, "Ensemble averaged surface normal impedance of material using an *in-situ* technique: Preliminary study using boundary element method," J. Acoust. Soc. Am. **125**(6), 3784–3791 (2009).
[31]J. F. Vincent and U. G. Wegst, "Design and mechanical properties of insect cuticle," Arthropod Struc. and Dev. **33**(3), 187–199 (2004).
[32]K. J. Bathe, A. Iosilevich, and D. Chapelle, "An evaluation of the MITC shell elements," Comput Struc. **75**(1), 1–30 (2000).
[33]S. Brenner and R. Scott, *The Mathematical Theory of Finite Element Methods*, Vol. 15 (Springer Science and Business Media, Berlin, 2015).
[34]COMSOL Multiphysics® v. 5.4. www.comsol.com. COMSOL AB, Stockholm, Sweden.